Cetin Morris SONSINO

Overview of the State of the Art on Multiaxial Fatigue of Welds*)

Fraunhofer-Institute for Strength of Structures under Operational Loading (LBF), Darmstadt / Germany

Key words: Welded joints, combined torsion and bending, constant and variable amplitude loading, in-and out-of-phase, nominal and local stresses, equivalent stress, damage accumulation

ABSTRACT: Flange-tube joints from fine grained steel StE 460 with unmachined welds were investigated under biaxial constant and variable amplitude loading (bending and torsion) in the range of 10^3 to $5 \cdot 10^6$ cycles to crack initiation and break-through, respectively. In order not to interfere with residual stresses they were relieved by a heat treatment. In-phase loading can be treated fairly well using the conventional hypotheses (von Mises or Tresca) on basis of nominal, structural or local strains or stresses. But the influence of out-of-phase loading on fatigue life is severely overestimated if conventional hypotheses are used. However, the introduced hypothesis of the effective equivalent stress leads to fairly well predictions. Herefore, the knowledge of local strains or stresses is necessary. They are determined by boundary-elemente analyses in dependency of weld geometry. This hypothesis consider the fatigue-life reducing influence of out-of-phase loading by taking into account the interaction of local shear stresses acting in different surface planes of the material. Further, size effects resulting from weld geometry and loading mode were included. Damage accumulation under a Gaussian spectrum can be assessed for in- and out-of-phase combined bending and torsion using an allowable damage sum of 0.35.

NOTATION

Stresses

σ	bending or normal stress
τ	shear stress
æ*	normalized stress gradient

Strains

ε	axial, bending or normal strain
γ	shear strain

Indexes

a	amplitude
a, b, t	axial, bending, torsion
arith	arithmetic
eq	equivalent
E	endurance
n	nominal, normal
m	mean
x, y, z	coordinates

*) This paper is an extended version of a contribution presented during the International Conference on Performance of Dynamically Loaded Welded Structures on July 14 and 15, 1997 in San Francisco.

Other symbols

D damage sum
E Young's modulus
G sliding modulus, ratio of stress concentration factors or of normalized stress gradients
K_t Stress concentration factor
N cycle
P_S probability of survival
R stress ratio
T scatter
f frequency
f_G size effect factor
k slope of S-N curve
$\tilde{k}$ slope of prolonged S-N curve
t time, depth
φ angle of an interference plane
δ phase angle
μ Poisson's constant
ω angular velocity ($2 \pi f$)

Introduction

Multiaxial random fatigue has been ignored by engineers for long times, despite the fact that fatigue critical areas like weld toes of many structures, e.g. Figs. 1, 2, 3, are subjected to multiaxial states of stress / strain. The latter do not result only from local constraints (stress concentrations) but can be caused also by multiaxial external loading like combined bending and torsion. The most complex local multiaxial stress / strain states are those with varying directions of principal stress / strain directions under random loading.

The designer is confronted with following problems in the assessment of multiaxial stress / strain states:

- Which kind of stresses / strains (nominal, hot-spot, structural, local) should be used?
- Which hypothesis should be used for the transformation of the multiaxial state into an equivalent one (von Mises or a modification)?
- Can design S-N curves obtained under uniaxial loading be applied for the assessment of multiaxial loading?
- Which damage accumulation hypothesis (Palmgren -Miner or a modification) and which allowable damage sum ($\Sigma\ (n/N)_i \leq D_{al}$, $D_{al} = 1.0$ or smaller) should be used in case of random multiaxial loading?

The paper will outline briefly the state of the art for the assessment of multiaxial fatigue of welds including design codes, will demonstrate on hand of some examples the problems and show possible solutions.

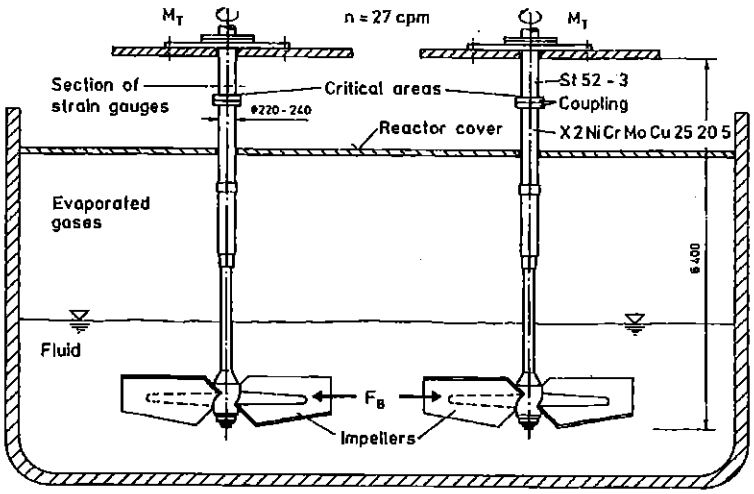

Fig. 1: Stirrers of a fertilizer plant

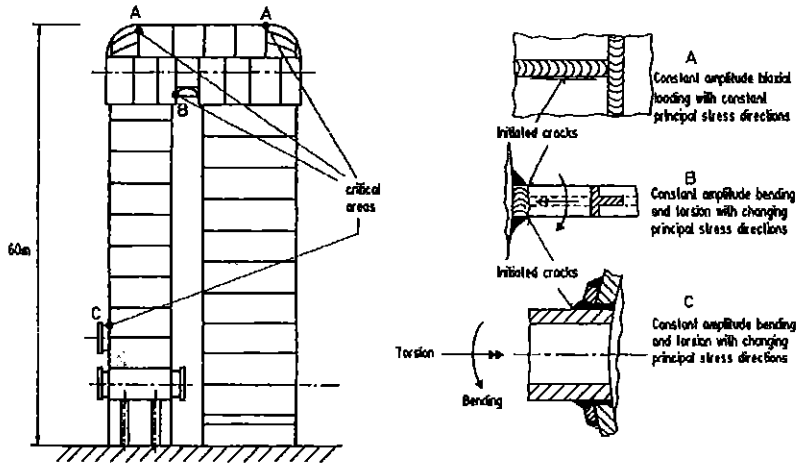

Fig. 2: Hot-blast furnace and critical areas

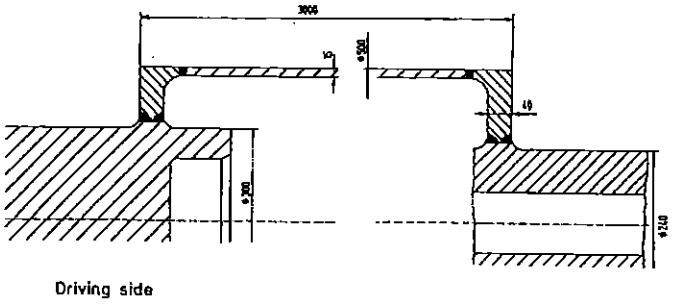

Fig. 3: Fatigue critical areas of a welded stirrer

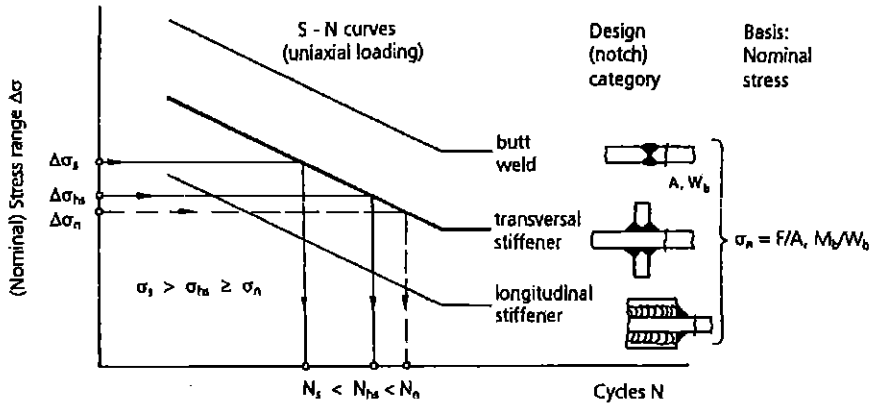

Maximum local notch stress can not be introduced into the nominal system!

Fig. 4: Fatigue evaluation concept in design codes using the nominal system

Short overview of different fatigue evaluation concepts

Definition of stress categories (nominal, hot-spot, structural, local)

There exist different concepts for the evaluation of the fatigue strength of welded structures. The most common concept is the nominal one. Generally, all design codes for welded structures base on this concept [1 to 7 a.o.]. Provided that a nominal stress can be defined,it is assigned to the design curve of the particular geometry (design category), Fig.4. These design curves are mostly obtained from uniaxial loading; the failure criterion is total failure. The different safety concepts (probability of failure) are not discussed in this paper.

The design curves presented on basis of nominal stresses are used also for two other concepts, namely the hot-spot [7, 8] and the structural stress concept [9], Fig. 5. The hot-spot stress is a fictional value derived by linear extrapolation of a calculated or measured stress-distribution to the weld toe. For structures where a nominal stress can be calculated by the use of basic mechanical equations like $\sigma_n = F/A$ or M_b / W_b the hot-spot stress is equal to the nominal stress. However, the structural stress close to the weld toe is significantly higher than the nominal or hot-spot ones, because it is also influenced by the geometrical transition due to the weld and the local notch effect, Fig. 5, left. If the structural stress, e. g. measured or calculated at a distance of 1 to 2 mm of the weld toe [9], is assigned to the particular design category, the fatigue life will be smaller than for the hot-

spot or nominal stress, Fig. 4. (The conservative result can be corrected, if the S-N curve is not presented in dependency of the nominal stress but of the structural stress at a defined distance to the weld toe.)

Recently, different variants of local concepts were applied to welds, too [12 to 20]. The basic idea is treating the weld as a notch and calculating the local stress distribution in the weld toe, Fig. 5, right. The notch (principal-) stress distribution is nothing else than the continuation of the structural stress distribution. The ratio between the maximum local (principal-) stress and the nominal or hot-spot stress corresponds to the theoretical stress-concentration factor K_t. The maximum local stress in the weld toe is the decisive value dominating the fatigue life.

For the case of uniaxial loading and the use of nominal, hot-spot or structural stresses the knowledge of the local stress is not mandatory as long as the used design curve is known for the assessed weld detail in the nominal system. But for combined multiaxial loading the knowledge of the particular maximum local stress components and of the nominal design curve is not sufficient, because the nominal stress components, e.g. for bending σ_n and for torsion τ_n, do not describe the local situation.

Fig. 6 shows the calculated stress-distributions for bending and torsion of a welded flange-tube connection [18, 19]. The stress raising effect of the notch is under bending more pronounced than for torsion.

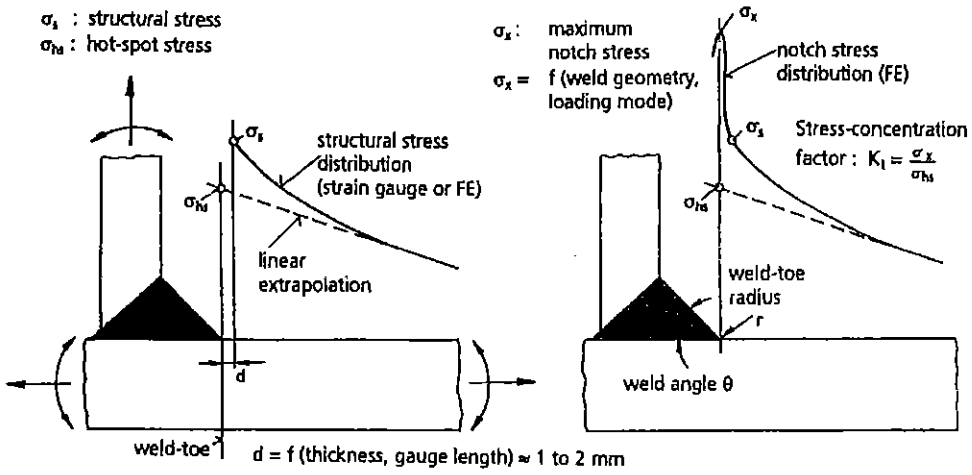

Fig. 5: Definition of stresses in a weld

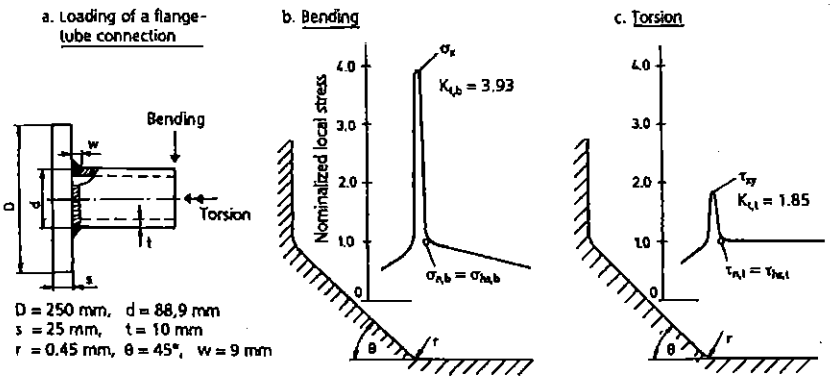

The exeedance of the nominal stress depends on the loading model

Fig. 6: Loading mode and stress concentration factors of a weld

Transformation of design curves from the nominal into the local system

Therefore, the nominal design curve must be transformed into a local one. The nominal design curve is shifted into the local curve, Fig. 7, by determination of the theoretical stress-concentration factor K_{tb} for bending and K_{tt} for torsion, e.g. by finite or boundary element calculations or from analytical solutions [10 to 13], and by the application of the von Mises equivalent stress criterion valid for ductile material state.

Under uniaxial loading (bending or axial) in the weld toe a biaxial stress state with the local stress components σ_x and σ_y is produced. The local equivalent stress according to the von Mises hypothesis which is suggested in several design codes for ductile materials reads with

$$\sigma_x = K_{tb} \cdot \sigma_n \text{ and} \tag{1}$$

$$\sigma_y = \mu \cdot \sigma_x \text{ for } K_{tb} > 2 \text{ [21]} \tag{2}$$

$$\sigma_{eq} = \sqrt{\sigma_x^2 + \sigma_y^2 - \sigma_x \cdot \sigma_y} = K_{tb} \cdot \sigma_n \cdot \sqrt{1 - \mu + \mu^2} \tag{3}$$

In case of uniaxial torque, the local equivalent stress is with

$$\tau_{xy} = K_{tt} \cdot \tau_n \tag{4}$$

$$\sigma_{eq} = \sqrt{3}\, K_{tt} \cdot \tau_{xy} \ . \tag{5}$$

If a shear stress is imposed to the bending due to an additional torsion, the equivalent stress is then extended to

$$\sigma_{eq} = \sqrt{\sigma_x^2 + \sigma_y^2 - \sigma_x \cdot \sigma_y + 3 \cdot \tau_{xy}^2} \quad (6)$$

Fig. 8 demonstrates an example for the assessment of a multiaxial stress state. The incorrect use of combined nominal stress components results in an underestimation of fatigue life, because the effect of the shear stress in relation to the normal stress is overestimated. Therefore, the correct evaluation of a multiaxial stress state requires the use of the physically decisive maximum local stress components.

However, the physically correct use of local maximum stresses does not always result in a correct equivalent stress if the von Mises hypothesis is applied. This hypothesis is only valid for proportional (in phase) multiaxial loading with not changing principal stress directions [18, 19]. Next section will indicate how to overcome the limitations of the von Mises criterion.

Assessment of multiaxial stress states

Constant amplitude loading

Experimental

In design codes mostly the application of the von Mises hypothesis is recommended on basis of nominal, hot-spot or structural stresses depending on the stress calculation method, but not on base of local notch stresses (or strains). Experiments were carried out with as welded and stress relieved, unmachined flange-tube connections from the structural fine-grained steel StE 460, Fig. 9. The failure criterion was the break-through of the tube, Fig. 10. Following results were obtained:

When a combined in-phase bending and torsion (nominal shear stress was selected to be 58 % of nominal bending stress) with constant principal stress directions is applied, the fatigue life can be assessed using any of the mentioned stress concepts, Fig.11. But for out-of-phase loading which simulates the changing of principal stress directions these concepts fail when the von Mises hypothesis is applied; this hypothesis overestimates the fatigue life severely, Fig. 11.

In order to overcome the deficiencies of this conventional hypothesis, a local stress based modification of von Mises, the hypothesis of effective equivalent stress (EESH) was developed [18, 19].

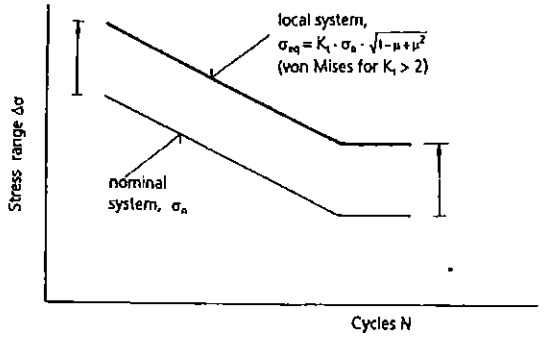

Fig. 7: Transformation of an S-N curve from the nominal into the local system

a. Nominal system

$\Delta\sigma_n = 100$ MPa

$\Delta\tau_n = 58$ MPa

$\Delta\sigma_{n,eq} = \sqrt{\Delta\sigma_n^2 + 3\Delta\tau_n^2}$ (von Mises)

$\Delta\sigma_{n,eq} = 141$ MPa

b. Local system ($K_{tb} = 3.93$; $K_{tt} = 1.85$)

$\Delta\sigma_x = K_{tb} \cdot \Delta\sigma_n = 393$ MPa

$\Delta\sigma_y = \mu \cdot \Delta\sigma_x = 118$ MPa

$\Delta\tau_{xy} = K_{tt} \cdot \Delta\tau_n = 107$ MPa

$\Delta\sigma_{loc,eq} = \sqrt{\Delta\sigma_x^2 + \Delta\sigma_y^2 - \Delta\sigma_x \cdot \Delta\sigma_y + 3\Delta\tau_{xy}^2}$

$\Delta\sigma_{loc,eq} = 395$ MPa

c. Evaluation

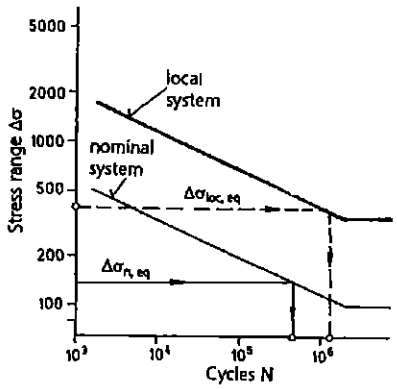

Fig. 8: Example for the assessment of a multiaxial stresses state

a. Specimen and clamping

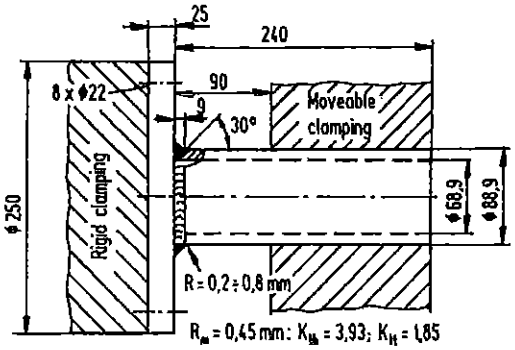

$R_m = 0{,}45$ mm: $K_{tb} = 3{,}93$; $K_{tt} = 1{,}85$

Material: StE 460, $R_m = 670$ MPa, $R_{p\,0,2} = 520$ MPa

Welding: MAG, stress-relief annealed

Hardness: Base material 200 HV 1, weld 320 HV 1

b. Microstructure

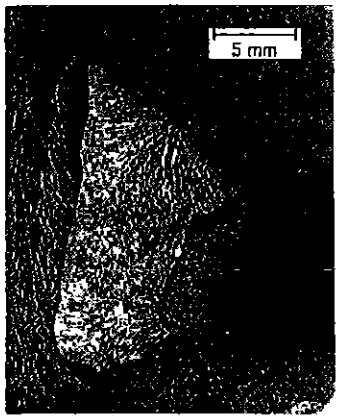

Fig. 9: Unmachined flange-tube-connection

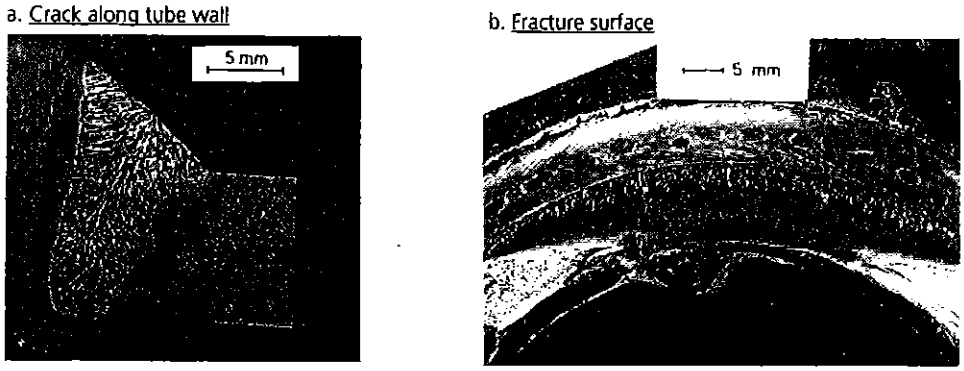

Fig. 10: Fracture of a welded flange-tube-connection

Effective equivalent stress hypothesis (EESH)

The local components of the stress tensor for the most common biaxial stress state

$$[\sigma] = \begin{bmatrix} \sigma_x & \tau_{xy} \\ \tau_{xy} & \sigma_y \end{bmatrix} \tag{7}$$

generated by sinusoidal combined bending and torsion read in general form in the weld toe (notch ground surface) as:

$$\sigma_x(t) = \sigma_{xm} + \sigma_{xa} \sin \omega_x t \,, \tag{8}$$

$$\sigma_y(t) = \sigma_{ym} + \sigma_{ya} \sin(\omega_y t - \delta_y) \,, \tag{9}$$

$$\tau_{xy}(t) = \tau_{xym} + \tau_{xya} \sin(\omega_{xy} t - \delta_{xy}) \tag{10}$$

In case of fully reversed stress (R = -1) the local mean stresses are σ_{xm}, σ_{ym} and $\tau_{xym} = 0$. The coordinate stresses σ_x and σ_y depend on each other, see equations (1) and (2), and are synchronous, i.e. $\delta_y = 0$. Only the shear stress is imposed with a phase displacement $\delta = \delta_{xy}$. The frequency of the tests discussed in this paper was kept the same for all stress components: $\omega = \omega_x = \omega_y = \omega_{xy}$. With this data the stresses acting in various interference planes φ of a surface element, Fig. 12, can be calculated:

$$\sigma_n(\varphi) = \sigma_x \cos^2\varphi + \sigma_y \sin^2\varphi + 2\,\tau_{xy} \cos\varphi \sin\varphi \text{ and} \tag{11}$$

$$\tau_n(\varphi) = \tau_{xy}(\cos^2\varphi - \sin^2\varphi) - (\sigma_x - \sigma_y)\cos\varphi \sin\varphi. \tag{12}$$

The EESH assumes that failure of ductile materials under multiaxial stress states is initiated by shear stresses $\tau_n(\varphi)$. The interaction of shear stresses in various interference

planes φ, in particular in the case of time-variable principal stress directions, which initiate corresponding dislocations, is taken into account by generating an effective shear stress

$$\tau_{arith} = \frac{1}{\pi}\int_0^{\pi} \tau_n(\varphi)\, d\varphi \qquad (13)$$

The effective shear stress is then used for determining the effective equivalent stress:

$$\sigma_{eq}(\delta) = \sigma_{eq}(\delta = 0°)\ \frac{\tau_{arith}(\delta)}{\tau_{arith}(\delta = 0°)}\ \sqrt{G \exp\left[1 - \left(\frac{\delta - 90°}{90°}\right)^2\right]}\ , \qquad (14)$$

$$\text{with} \quad \sigma_{eq}(\delta = 0°) = \sqrt{\sigma_x^2 + \sigma_y^2 - \sigma_x\sigma_y + f_G^2\, 3\, \tau_{xy}^2}\ , \qquad (15)$$

$$f_G = \frac{\sigma_{eq,DEH\ (pure\ axial\ or\ bending\ load)}}{\sigma_{eq,DEH\ (pure\ torsion)}} = \frac{\sqrt{\sigma_x^2 + \sigma_y^2 - \sigma_x\sigma_y}}{\sqrt{3}\cdot\tau_{xy}}\ , \qquad (16)$$

$$\text{and} \quad G = \frac{1+K_{ta}}{1+K_{tt}} \ \text{or}\ \frac{1+K_{tb}}{1+K_{tt}} \ \text{or}\ \frac{1+\ae_a^*}{1+\ae_t^*} \ \text{or}\ \frac{1+\ae_b^*}{1+\ae_t^*}\ . \qquad (17)$$

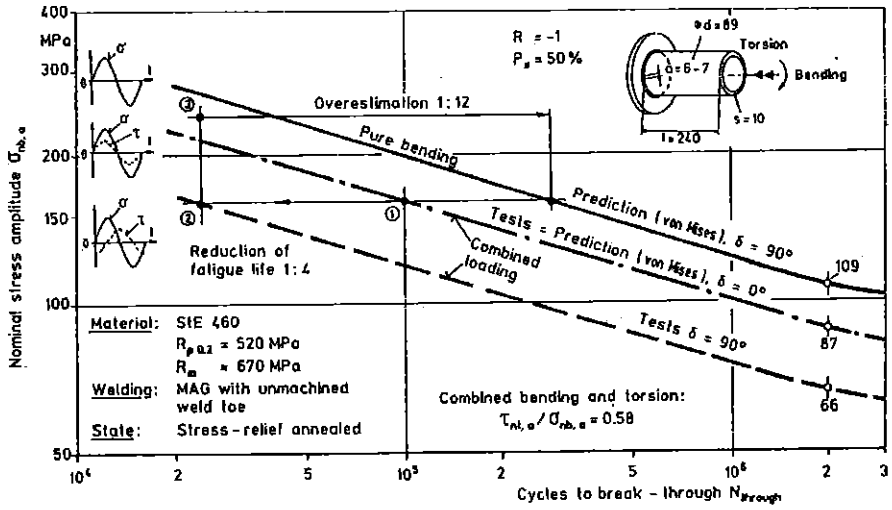

Fig. 11: Fatigue strength of welded unmachined flange-tube-connections under multiaxial loading

Here, f_G is the size effect factor which is determined by comparing the S-N curve for pure axial or bending stress with that for pure torsion on the basis of local supportable stresses. This factor reflects the influence of the maximum stressed material volume on the supportable local stress. The root in equation (14) considers the influence of the material volume affected by the rotating principal stress and principal strain axes on the magnitude

of the effective equivalent strain in the case of a phase displacement according to a model developed for semiductile materials. The ratio G in the equations (14) and (17) can be computed with the corresponding stress concentration factors. In the case of complex geometries, however, the corresponding stress gradients can, for instance, be found by a finite element computation and the referenced normalized stress gradients

$$\text{æ}^* = \frac{1}{\sigma_{x,max}} \cdot \frac{d\sigma_x}{dx} \tag{18}$$

can thus be determined. The basis for the effective equivalent stress is given by the appropriate S-N curve for pure bending load. The local coordinate stresses are calculated from the nominal stress and the stress concentration factor according to the equations (1) and (2) and used for calculating the local equivalent stress according to the equation (3).

For evaluating the multiaxial stress state, the effective equivalent stress calculated according to equation (14) is then allocated to the reference S-N curve thus derived.

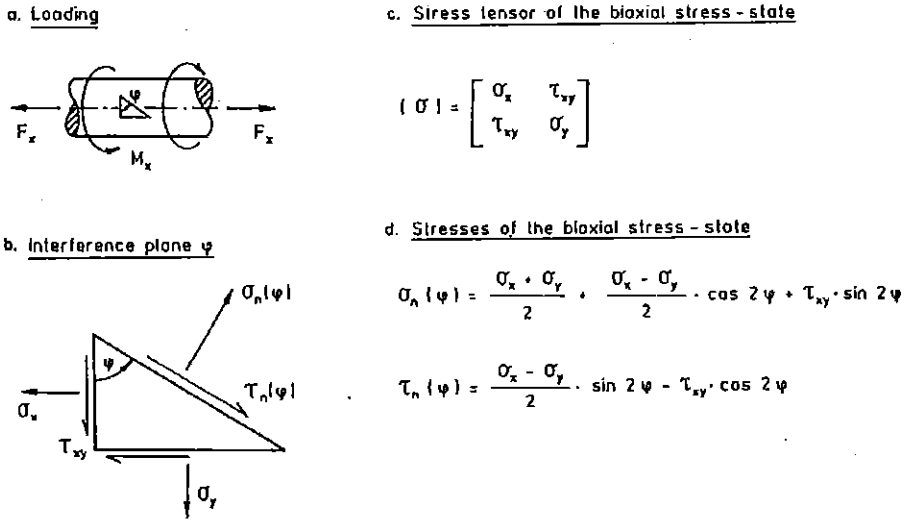

Fig. 12: Interference plane stresses

Evaluation of results for welded flange-tube connections

Fig. 13 shows the reference S-N curve with the scatter band between P_S = 10 and 90 % for the unmachined flange-tube connections. This curve reflects the interdependence of the local equivalent stress amplitude according to equation (3) and the cycles to the

performed under pure bending, pure torsion and with combined in-phase and out-of-phase loading lie within the scatter band of the reference S-N curve if they were derived according to the EESH.

This hypothesis was applied successfully also to other welded joints, such as to machined flange-tube connections having lower stress concentrations than unmachined ones, to unmachined and machined tube-tube connections, all subjected to combined constant amplitude in- and out-of-phase bending and torsion [18, 19].

The question that arises is, if the EESH will be applicable also to variable in- and out-of-phase amplitude loading. For answering this question, first the cumulative fatigue behaviour [22] of the welded connections under uniaxial bending and torsion must be known.

Cumulative fatigue behaviour under uniaxial bending and uniaxial torsion

Damage accumulation

The cumulative fatigue life of welded connections is generally calculated according to the Palmgren-Miner rule

$$\sum \left(\frac{n}{N}\right)_i \leq D \quad . \tag{19}$$

According to Haibach [23] after the knee point (this can be assumed for welded steels at $2 \cdot 10^6$ cycles or more) the inclination $\overline{m}$ of the S-N curve becomes shallower than its inclination k before the knee point:

$$\overline{m} = 2\,k - 1. \tag{20}$$

In most design codes for the damage sum the value D = 1.0 is prescribed. Based on different experiences under uniaxial loading the value of D = 0.5 seems to be more realistic [24, 25]. However, information on realistic damage sums under combined multiaxial random loading is until now not available. It is even not known whether damage sums obtained under uniaxial random loading can be used for the assessment of multiaxial random loading. Therefore, a systematic investigation was carried out [26] beginning with the determination of damage sums for uniaxial random bending and uniaxial random torsion applied to welded unmachined, stress-relieved flange-tube specimens, Fig. 9, and then extended to multiaxial random loading. (At time different

research projects about this topic [26, 27] are running in Germany.)

Results of uniaxial spectrum loading

The tests were carried out under a Gaussian spectrum of amplitudes with a sequence length of $L_S = 5 \cdot 10^4$ cycles, Fig. 14 [26].The failure criterion was again the break-through of the tube. Figs. 15 and 16 show the fatigue-life curves obtained under uniaxial random bending and uniaxial random torsion; the nominal stress amplitude presented is the maximum value of the spectrum. Figs. 15 and 16 contain also the results determined under constant amplitude loading.

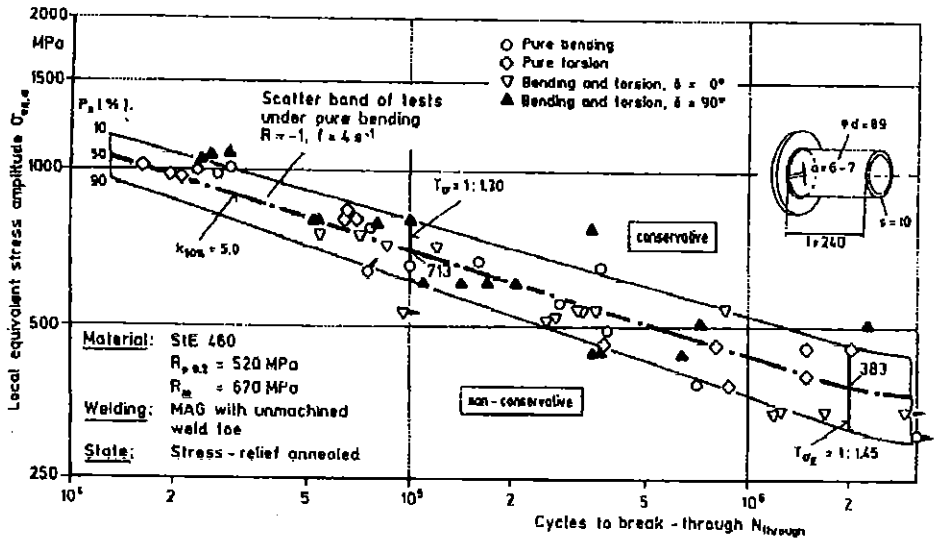

Fig. 13: Evaluation of multiaxial stress states with the hypothesis of effective equivalent stress (EES) for welded, unmachined flange-tube connections

For a given fatigue life, e.g. at $N = 2 \cdot 10^6$ cycles, the ratio between the endurable maximum stress amplitude of the spectrum and the constant stress amplitude is for torsion higher than for bending, factor 2.16 vs 1.64. This indicates different damage sums for the particular loading. The determination of the real damage sums

$$D_{real} = \frac{\overline{N}_{experiment,Ps=50\%}}{\overline{N}_{calculated(D=10)}} \qquad (21)$$

according to the equations (19) and (20) results for bending $D_{real,b} = 0.08$ and for torsion $D_{real,t} = 0.38$, Table 1a.

a. Amplitude distribution

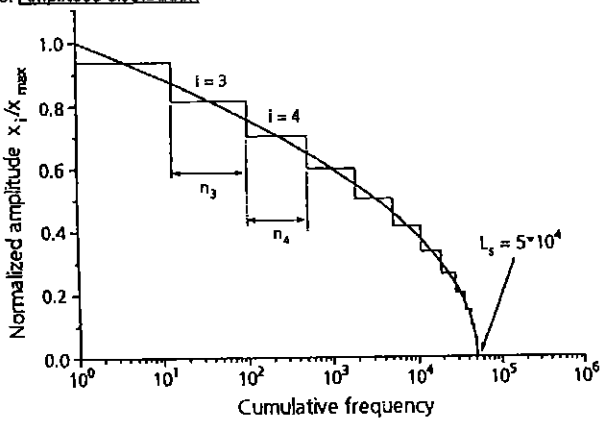

b. Stepping of the spectrum

i	x_i	n_i
1	1.000	1
2	0.938	12
3	0.817	87
4	0.704	418
5	0.600	1377
6	0.504	3256
7	0.417	5768
8	0.337	7964
9	0.267	8859
10	0.204	8156
11	0.150	6325
12	0.104	4158
13	0.067	2285
14	0.037	997
15	0.017	299
16	0.004	38
	$\Sigma n_i = H_s = 50000$	

Fig. 14: Gaussian spectrum with sequence length $L_s = 5 \cdot 10^4$ cycles

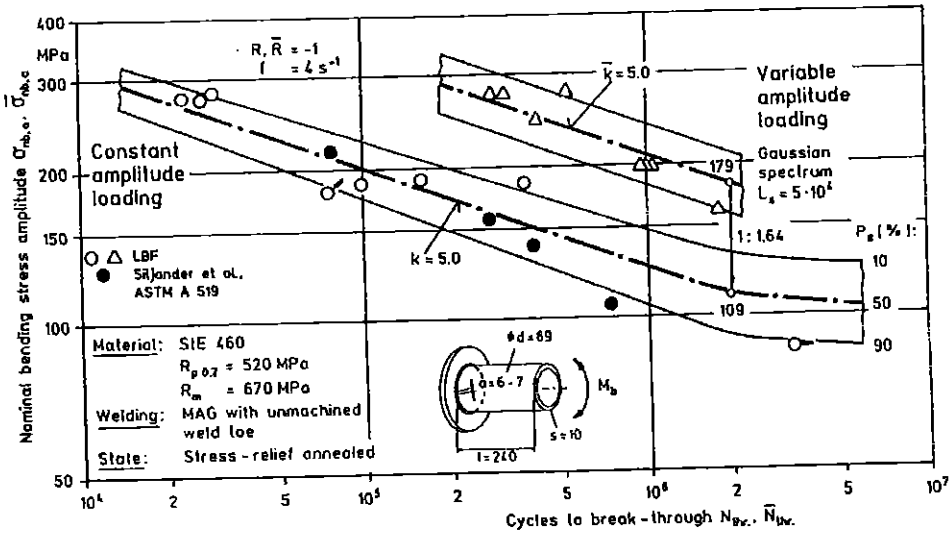

Fig. 15: Fatigue strength of welded unmachined flange-tube-connections under uniaxial constant and variable amplitude bending

The different damage sums for uniaxial random bending and uniaxial random torsion justify the necessity for investigations under combined multiaxial in- and out-of-phase random loading in order to obtain the appropriate D_{real}.

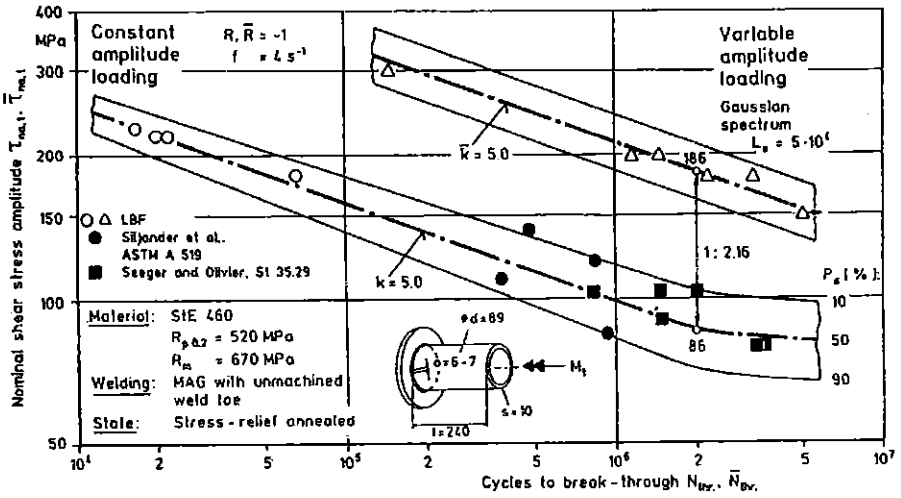

Fig. 16: Fatigue strength of welded unmachined flange-tube-connections under uniaxial constant and variable amplitude torsion

Cumulative fatigue behaviour under multiaxial random loading

The tests under combined bending and torsion of flange-tube specimens will be carried out under Gaussian spectra with a sequence length of $L_S = 5 \cdot 10^4$ cycles. The bending and-torque-time histories will be applied in- and out-of-phase. The nominal shear stress will be according to the von Mises hypothesis ($\tau_n/\sigma_n = 1/\sqrt{3}$) 58 % of the nominal bending stress.

Fig. 17 presents the test results obtained from constant amplitude in- and out-of-phase multiaxial loading as basis for the damage accumulation calculation. (Fig. 11 contains the mean curves with $P_s = 50$ %.)

In Fig. 18 the curves determined from random in- and out-of-phase multiaxial loading are shown. Also under random loading the changing of principal directions causes a significant decrease of fatigue life. The fatigue life in the medium-cycle range ($10^4 < N < 10^6$)is reduced by a factor of 4 like under constant amplitude multiaxial loading. Therefore, the EESH which described the multiaxial constant amplitude fatigue behaviour satisfactorily, Fig. 13, is also applicable to in- and out-of-phase multiaxial random loadings because of same slopes of the fatigue life curves and same fatigue life reduction factor.

Figs. 19 and 20 compare the appertaining constant and variable amplitude curves with $P_s = 50$ % for in- and out-of-phase loading.

For the fatigue life of $N = 2 \cdot 10^6$ cycles the multiaxial constant amplitudes are exceeded under in- as well as out-of phase multiaxial random loading by nearly same factor 2.11 to 2.12. The determined real damage sums according to the equations are $D_{real} = 0.35$ and 0.38, Table 1b.

Fig. 21 compares the obtained real damage sums for the investigated loading cases. However, the determined real damage sums for multiaxial random loading should not be generalized before testing other combinations of the bending and shear stresses.

Table 1: Real damage sums for variable amplitude loading of welded, unmachined flange-tube specimens under pure bending, pure torsion and combined in- and out-of-phase loading

a. Pure bending and pure torsion

Loading	Knee-point of the S-N curve $N_k(P_ü = 50\ \%)$	Endurance limit $(P_ü = 50\ \%)$ $\bar{\sigma}_E ; \bar{\tau}_E$ in MPa	Slope of the S-N curve k_{sam}	$k' = 2k-1$	$D_{Spectrum}$ $L_{Spectrum} = 5 \cdot 10^4$	Calculated life $\bar{N}_{cal}$ (D=1.0) for $\bar{\sigma}_{ra} ; \bar{\tau}_{ra} = 200$ MPa	Experimental life $\bar{N}_{exp}$ for $\bar{\sigma}_{ra} ; \bar{\tau}_{ra} = 200$ MPa	Real damage sum $D_{real} = \bar{N}_{exp} / \bar{N}_{cal}$
Bending	2 000 000	109	5.0	9.0	0.0034	14 618 060	1 148 500	0.078
Torsion	2 000 000	86	5.0	9.0	0.0138	3 621 334	1 391 400	0.384

b. Combined bending and torsion

Loading	Knee-point of the S-N curve $N_k(P_ü = 50\ \%)$	Endurance Limit $(P_ü = 50\ \%)$ $\bar{\sigma}_E$ MPa	Slope of the S-N curve k_{sam}	$k' = 2k-1$	$D_{Spectrum}$ $L_{Spectrum} = 5 \cdot 10^4$	Calculated life $\bar{N}_{cal}$ (D=1.0) for $\bar{\sigma}_{ra} = 200$ MPa	Experimental life $\bar{N}_{exp}$ for $\bar{\sigma}_{ra} = 200$ MPa	Real damage sum $D_{real} = \bar{N}_{exp} / \bar{N}_{cal}$
In-phase $\varphi = 0°$	2 000 000	87	5.0	9.0	0.0129	3 871 012	1 350 000	0.349
Out-of-phase $\varphi = 90°$	2 000 000	66	5.0	9.0	0.0567	890 320	338 000	0.380

$$D_{Spectrum} = \Sigma\left(\frac{n}{N}\right)_i \qquad D_{real} = \frac{D_{Spectrum}}{L_{Spectrum}} \cdot \bar{N}_{exp} = \bar{N}_{exp} / \bar{N}_{cal} \qquad \bar{N}_{cal} = \frac{L_{Spectrum}}{D_{Spectrum}}$$

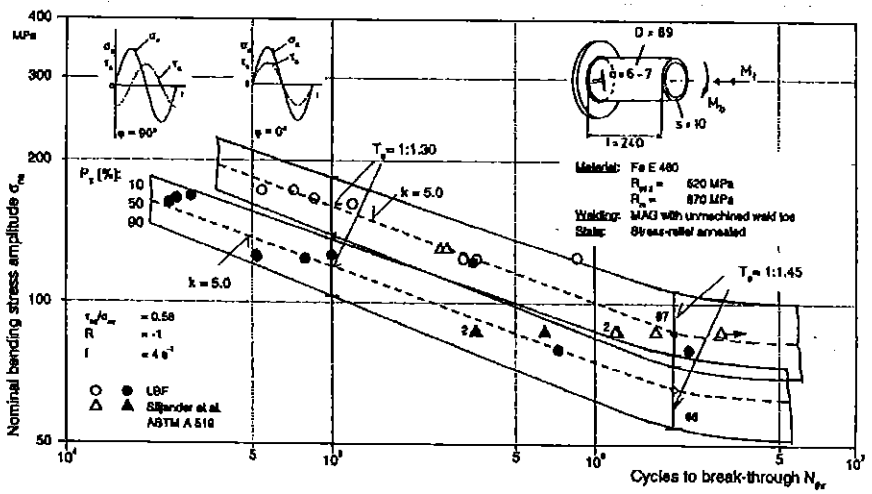

Fig. 17: Combined constant amplitude loading of welded, unmachined flange-tube specimens

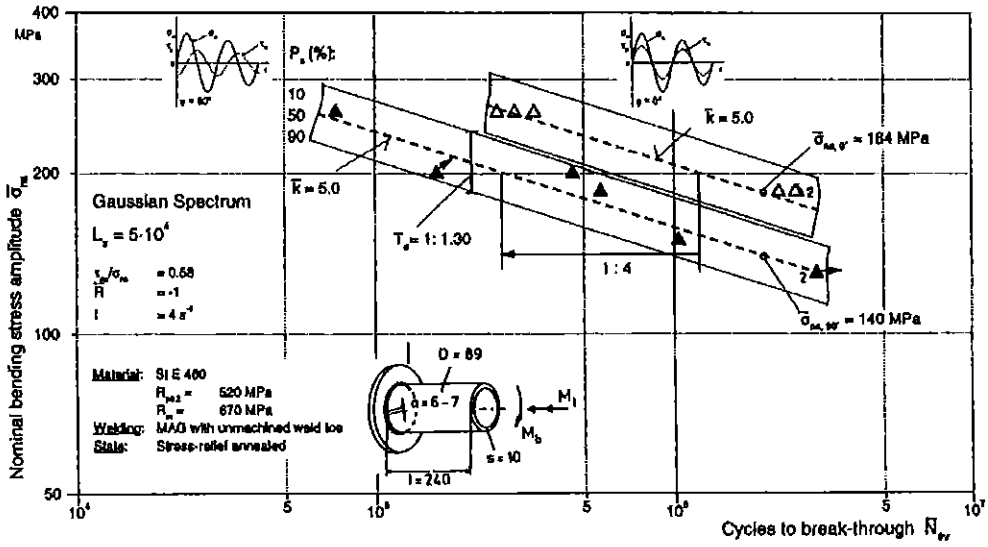

Fig. 18: Combined variable amplitude loading of welded, unmachined flange-tube specimens

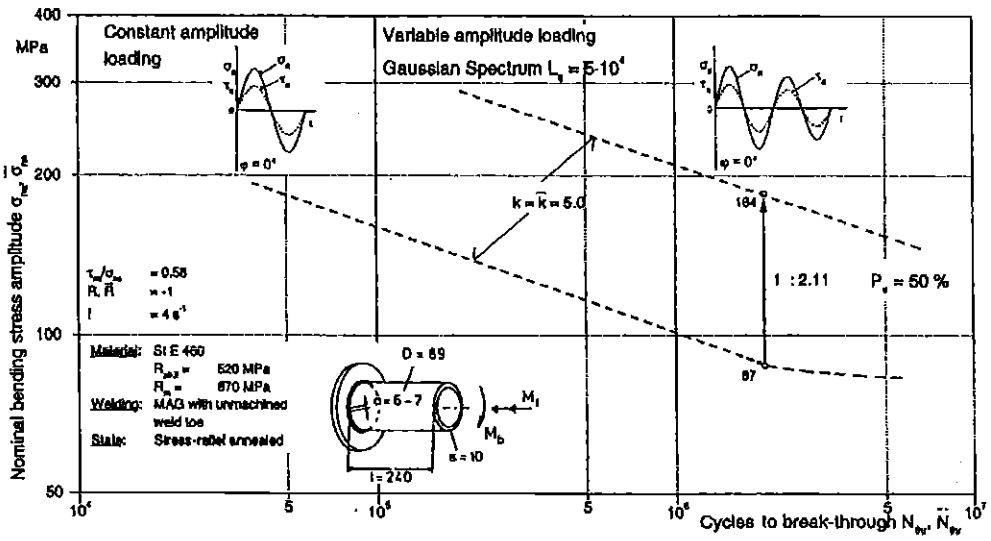

Fig. 19: Comparison of in-phase combined constant and variable amplitude loading of welded, unmachined flange-tube specimens

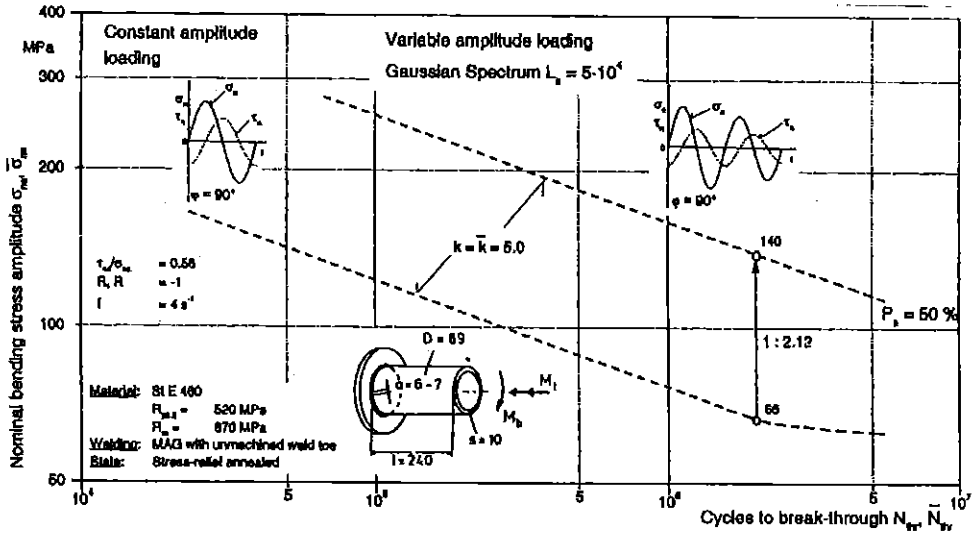

Fig. 20: Comparison of out-of-phase combined constant and variable amplitude loading of welded, unmachined flange-tube specimens

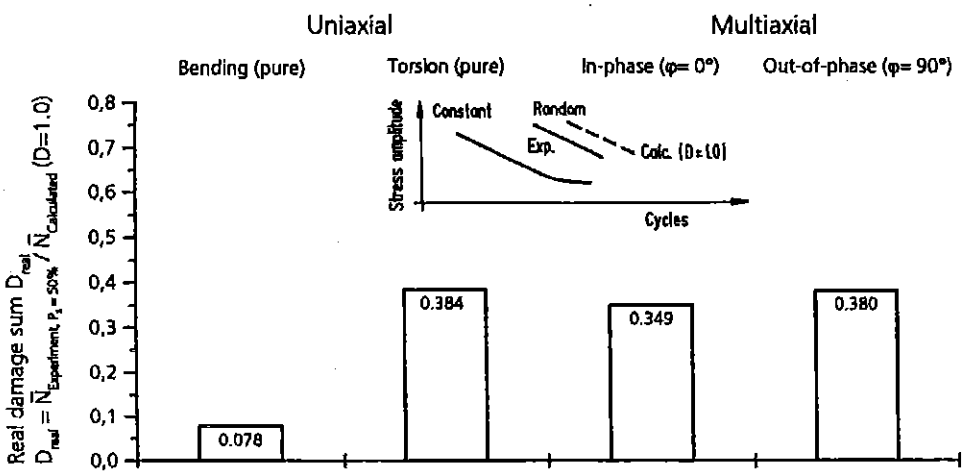

Fig. 21: Real damage sums for uniaxial and multiaxial random loading of welded, unmachined, flange-tube specimens

Assessment of cumulative fatigue life according to the EESH

Fig. 22 traces briefly how to apply the Effective Equivalent Stress Hypothesis (EESH) for the assessment of the cumulative fatigue life under multiaxial random loading, when the real damage sum D_{real} is known:

- The local stress time-histories $\sigma_x(t)$, $\sigma_y(t) = \mu \cdot \sigma_x(t)$ and $\tau_{xy}(t)$ and corresponding spectra with the maximum values $\bar{\sigma}_x$, $\bar{\sigma}_y = \mu \cdot \bar{\sigma}_x$ and $\bar{\tau}_{xy}$ are calculated using the nominal bending and shear stresses and the stress concentration factors for bending K_{tb} and torsion K_{tt}, respectively.
- From the local stress-time histories the shear stress time histories in different interference planes φ for the given phase angle δ between $\sigma_x(t)$ and $\tau_{xy}(t)$ are determined according to equation (12).
- For a given phase angle δ the shear stress spectrum in each plane φ is determined. By assigning the spectra to the uniaxial local shear stress-cycle curve the damage sums D (φ, δ) are calculated for each plane. Damage occurs in the plane φ^* where damage is maximum: D_{max} (φ^*, δ).
- As steel welds are ductile the interaction of shear stresses acting in different planes φ must be considered by calculation of the effective (arithmetic avarage) damage sum for in-phase loading $\delta = 0°$and for a given phase angle δ analogue to equation (13).
- The effective equivalent stress spectrum is determined while for the shape of this effective spectrum the shape of the shear stress spectrum with $D_{max}(\varphi^*, \delta)$ is taken. The maximum value of the effective equivalent spectrum is calculated using the maximum values of the input spectra according to the equations (14) to (17).
- Finally, the cumulative fatigue life under multiaxial random loading is calculated by assigning the effective equivalent spectrum to the local S-N-curve obtained from uniaxial bending. The calculated fatigue life

$$\bar{N}_{cal} = \frac{L_S}{D_{eff}} \cdot D_{real} \qquad (22)$$

must be connected with the real damage sum D_{real} which is obtained from presented multiaxial random tests.

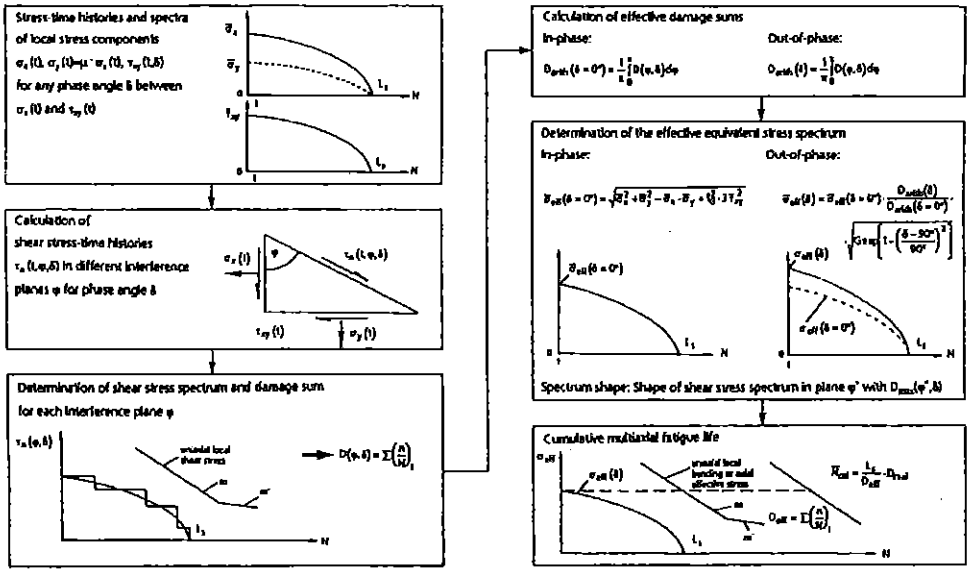

Fig. 22: Application of the effective equivalent stress hypothesis to multiaxial random loading

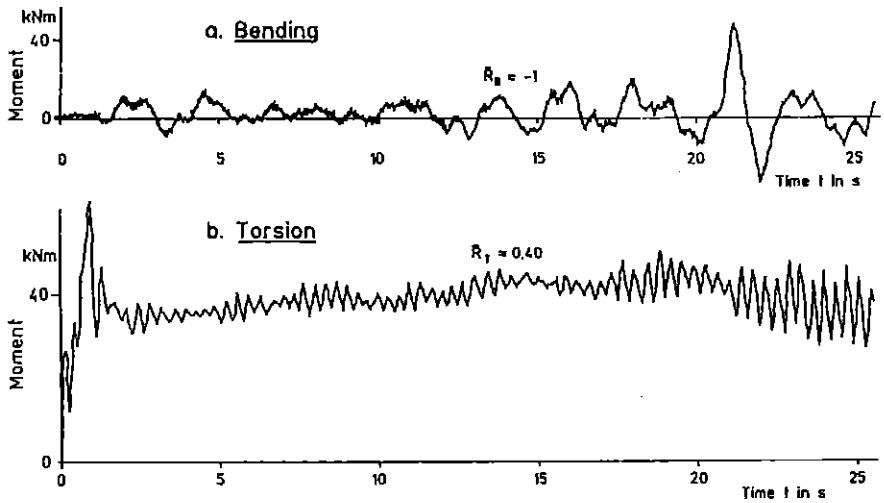

Fig. 23: Multiaxial random-load-time-histories

Present recommendations

Allthough not all necessary clarifying knowledge from research presently performed on multiaxial random fatigue [26, 27] is yet available, i.e. the obtained real damage sums for multiaxial random loading cannot yet be generalized, some

recommendations can be given for dimensioning of welded structures against such complex loading situations:

- It is necessary to determine the local stress-time histories of the stress components. As the local values cannot be measured, it is sufficient if structural stresses σ_{sx}, σ_{sy}, τ_{sxy} are measured and then transformed by stress concentration factors K_{tb}, K_{tt} into local values σ_x, σ_y, τ_{xy}. If stress concentration factors are not available, a boundary or finite element modelling can be helpful.
- In structures random torsion and bending stresses can differ very much with regard to frequencies and spectrum shapes. Fig. 23 shows such bending- and torque-time histories measured at the shaft of a fertilizer stirrer, Fig. 1 [28]. The bending stresses are fluctuating (R = -1), while the torsion is a start-stop event with small fluctuations about a positive mean stress.
- The particular spectra are presented on Fig. 24. In the weld toe shear stresses could be calculated for different interference planes φ according to equation (12), and effective damage sums could be determined. As for this complex load situation the knowledge for assessment is still not available a practical way to solve the problem with conservative assumptions can be proposed:
- The influence of different mean bending and shear stresses, Fig. 24, is corrected by application of the mean stress sensitivity of the steel used. The shear stress is transformed to the stress ratio R = -1 of the bending stress. The shape and size of the effective equivalent stress spectrum is determined by the spectrum shape of the most intensive local stress component. In this case it is the bending stress which has a fuller shape in comparison to the shear stress spectrum.
- This means as if the torsion would fluctuate with the same frequency of the bending moment and additionally has the shape of the bending spectrum; i.e. the shear stress would act in a more damaging (intensive) way as in reality.
- The maximum effective equivalent stress is obtained by application of the EESH. A constant amplitude in- and out-of-phase simulation with the maximum bending and shear stresses of the corresponding spectra is carried out with the most critical phase angle of $\delta = 90°$ for ductile steels.
- The effective spectrum is then assigned to the local S-N curve of the welded design

detail, Fig. 25.

- The cumulative fatigue life is calculated assuming an allowable damage sum of $D_{al} = 0.50$.

The stirrers discussed here, Fig. 1, were redesigned, Fig. 25, fifteen years ago after several structural failures applying very conservative assumptions [28]. (After the redesign of the shafts no failures occured.) The use of the present knowledge on multiaxial fatigue results in a similar effective equivalent stress spectrum. However, the extent of conservatism introduced can be evaluated only when more detailed results on multiaxial random fatigue will be available.

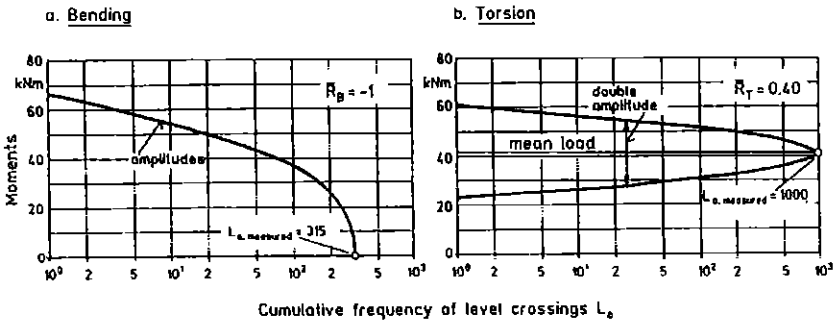

Fig. 24. Cumulative frequency distributions

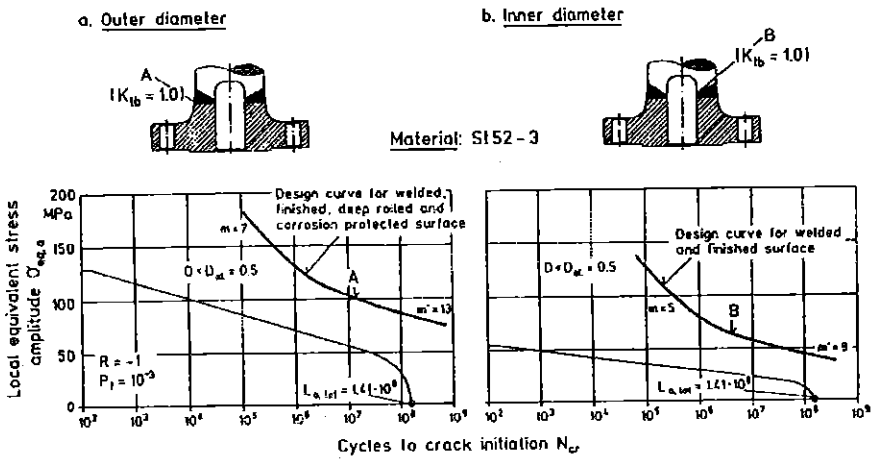

Fig. 25: Fatigue life evaluation of the final design of the stirrer coupling

Conclusions and outlook

Principally, the evaluation of constant or variable (random) amplitude multiaxial fatigue of welds requires the knowledge of the local stress state in the weld toe (notch). It can be determined by boundary or finite element modelling of the weld detail. The observed fatigue life reduction of ductile steel welds under constant and random amplitude multiaxial loading with changing principal stress directions compared with welds with constant principal directions, e.g. simulated by out-of-phase and in-phase bending and torsion, can be described fairly well by the Effective Equivalent Stress Hypothesis (EESH). While uniaxial random bending and random torsion tests reveal different real damage sums ($D_{real,b}$ = 0.38, $D_{real,t}$ = 0.08) the value of the real damage sum for cumulative multiaxial fatigue assessments was found to be D_{real} = 0.35 to 0.38. However, a systematical investigation of multiaxial random fatigue, as it is presently performed [26, 27], is necessary, because the obtained real damage sum cannot yet be generalized. Despite conservative recommendations how to use existing knowledge for the assessment of multiaxial random loading of welds validation tests must be carried out in critical cases.

The multiaxial fatigue research comprises presently steel welds, which have ductile material behaviour. From present knowledge on multiaxial fatigue behaviour of unwelded materials it can be concluded that aluminium welds, which are not as ductile as steel, may require the application of other stress and cumulative damage hypotheses. A new research project about the multiaxial fatigue behaviour of aluminium welds is also in progress.

Fracture mechanics concepts [29 to 32] have not yet been applied to multiaxial fatigue problems in order to predict crack propagation. The project [28] in progress also aims at applicable fracture mechanics concepts.

References

[1] EUROCODE Nr. 3, Gemeinsame einheitliche Regeln für Stahlbauten, Kommission der Europäischen Gemeinschaften, Stahlbau-Verlagsgesellschaft mbH, Köln (1992)

[2] British Standard BS 5400, Steel, Concrete and Composite Bridges, Part 10, Code of Practice for Fatigue, BSI (1980)

[3] ASME Boiler and Pressure Vessel Code, Section III, Division 1, Subsection NA, Article XIV-1212, Subsection NB-3352.4, New York (19984)

[4] AD-Merkblatt S 2, Berechnung gegen Schwingbeanspruchung, Beuth-Verlag,

Berlin/Köln (1982)

[5] DS 804, Vorschrift für Eisenbahnbrücken und sonstige Ingenieurbau-werke (VEI), Deutsche Bahn, Munic (1996)

[6] Hobbacher, A., Recommendations on Fatigue of Welded Components, IIW Fatigue Design Recommendation, IIW-Document No. XIII-1539-94/XV 845-94 (1994)

[7] Niemi, E., Stress Determination for Fatigue Analysis of Welded Components, Abington Publishing, Cambridge (1995)

[8] De Back, J., Festigkeit von Rohranschlüssen, In: Stahl in Meeresbau-werken, Internationale Konferenz 5.-8.10.19981, Paris, Hrsg.: Kommission der Europäischen Gemeinschaften, Luxemburg: EUR-Bericht No. 7347 (1981), pp. 439 - 483

[9] Haibach, E., DieSchwingfestigkeit von Schweißverbindungen aus der Sicht einer örtlichen Beanspruchungsmessung, Fraunhofer-Institut für Betriebs-festigkeit (LBF), Darmstadt, Report No. FB-77 (1968)

[10] Yung, J.-H.; Lawrence, F.V., Analytical and Graphical Aids for the Fatigue Design of Weldments, Fatigue Fract. Eng. Mat. Struc. 8 (1985), No. 3, pp. 223 - 241

[11] Anthes, R.J.; Köttgen, V.B.; Seeger, T., Einfluß der Nahtgeometrie auf die Dauerfestigkeit von Stumpf- und Doppel-T-Stößen, Schweißen und Schneiden 46 (1994) No. 9, pp. 433 - 436

[12] Iida, K.; Uemura, T., Stress Concentration Factor Formulas Widely Used in Japan, IIW-Document No. XIII-1530-94 (1994)

[13] Radaj, D., Design and Analysis of Fatigue Resistant Welded Structures, Woodhead Publishing, Cambridge (1994)

[14] Yung, J.Y.; Lawrence, F.V. Jr., Predicting the Fatigue Life of Welds Under Combined Bending and Torsion, In: Biaxial and Multiaxial Fatigue, EGF 3, Ed. by M.W. Brown and K.J. Miller, Mechanical Engineering Publications, London (1989), pp. 53 - 69

[15] Lawrence, F.V. Jr.; Mattos, R.J.; Higashida, Y.; Burk, J.D., Estimating Fatigue Crack Initiation Life of Welds, In: ASTM STP 648 (1978), pp. 134 -158

[16] Siljander, A.; Kurath, P.; Lawrence, F.V. Jr., Proportional and Non-Proportional Mulit-Axial Fatigue of Tube-to-Plate Weldments, University of Illinois at Urbana-Champaign, Urbana, Illinois, Report to the Welding Research Council (1989)

[17] Siljander, A., Nonproportional Biaxial Fatigue of Welded Joints Dissertation Univ. Illinois (1991)

[18] Sonsino, C.M., Multiaxial Fatigue of Welded Joints under In-Phase and Out-of-Phase Local Strain and Stresses, International Journal of Fatigue 17 (1995) No. 1, pp. 55 - 70

[19] Sonsino, C.M., Multiaxial Fatigue of Welded Flange-Tube- and Tube-Tube Connections under In- and Out-of-Phase Loading and Local Stresses IIW-Document No. XIII-1542-94 (1994)

[20] Radaj, D., Review of Fatigue Strength Assessment of Nonwelded and Welded Structures Based on Local Parameters, International Journal of Fatigue 18 (1996) No. 3, pp. 153 --170

[21] Neuber, H., Kerbspannungslehre - Theorie der Spannungskonzentration, Genaue Berechnung der Festigkeit, Springer Verlag, Berlin (1985), 3. Edition

[22] Buxbaum, O., Betriebsfestigkeit - Sichere und wirtschaftliche Bemessung schwingbruchgefährdeter Bauteile, Verlag Stahleisen mbH, Düsseldorf, 2. Edition (1992)

[23] Haibach, E., Betriebsfestigkeit - Verfahren und Daten zur Bautei-berechnung, VDI-Verlag GmbH, Düsseldorf (1989)

[24] Sonsino, C.M., Über den Einfluß von Eigenspannungen, Nahtgeometrie und mehrachsigen Spannungszuständen auf die Betriebsfestigkeit geschweißter Konstruktionen aus Baustählen, Materialwissenschaft und Werkstofftechnik 25 (1994) No. 3, pp. 97 - 109

[25] Sonsino, C.M.; Umbach, R., Corrosion Fatigue of Welded and Cast-Steel Hybrid Nodes under Constant and Variable Amplitude Loading, In: Proceedings of the 12th Int. Conf. on Offshore Mechanics and Arctic Engineering, OMAE 1993, Glasgow, Ed. by M.H. Salama, S.E. Webster, J.V. Haswell, E.A. Patterson and P.J. Haagensen, American Society of Mechanical Engineers (ASME), New York, Vol. III, Part B (1993), pp. 667 - 674,

[26] Fatigue Behaviour of Welded High Strength Components under Combined Multiaxial Variable Amplitude Loading, European Community for Steel and Coal (ECSC), Contract 7210 MC/109, Fraunhofer-Institut für Betriebsfestigkeit (LBF), Darmstadt

[27] Research Project of the Deutsche Forschungsgemeinschaft (DFG), Fatigue Strength of Welded Connections under Multiaxial Loading (1995-1998)

[28] Sonsino, C.M.; Pfohl, R., Multiaxial Fatigue of Welded Shaft-Flange Connections of Stirrers under Random Non-Proportional Torsion and BendingInt. Journal of Fatigue 12 (1990) No. 5, pp. 425 - 431

[29] Maddox, S.J., Fatigue Strength of Welded Structures, Abington Publishing, Cambridge (1991)

[30] PD 6493, Guidance on Methods for Assessing the Acceptability of Flaws in Fusion Welded Structures, British Standards Institution - BSI, London (1991)

[31] DVS-Merkblätter 2401, Bruchmechanische Bewertung von Fehlern in Schweißverbindungen, Teil 1: Grundlagen und Vorgehensweise; Teil 2: Praktische Anwendung, Fachbuchreihe Schweißtechnik, Bd. 101 (1989), DVS-Verlag, Düsseldorf

[32] Hobbacher, A., Stress Intensity Factors of Welded Joints, Eng. Fracture Mech. 46 (1993) No. 2, pp. 173 - 182

Acknowledgement: The author thanks to Dr. S. Maddox (TWI) and Prof. Dr. O. Buxbaum (LBF) for reviewing this paper.